NWRI CONTRIBUTION 85-140

Engel (43)

DeZeeuw (12)

Study No. 85-332

IMPROVEMENTS TO THE LOW SPEED RESPONSE OF THE PLASTIC ROTOR FOR THE PRICE CURRENT METER - PHASE I

by

P. Engel[1] and K. Wiebe[2], R. Terzi[3], C. DeZeeuw[4]

[2] Head
[3] Standards Officer
Hydrometric Methods and Development Section
Water Survey of Canada
Water Resources Branch
Place Vincent Massey
Hull, Quebec

[1]Environmental Hydraulics Section
[4]Technical Services Section
Hydraulics Division
National Water Research Institute
Canada Centre for Inland Waters
Burlington, Ontario

November 1985

SUMMARY

Owing to the joint initiative of Water Survey of Canada and the Hydraulics Division of the National Water Research Institute, this study has been conducted to develop a plastic rotor for the Price meter with the best possible low speed performance. Preliminary designs have been obtained based on theoretical considerations and towing tank tests. Indications are that threshold velocities of less than 2 cm/s can be obtained. More extensive tests are planned to evaluate the consistency in the performance of the new rotor designs over a wider range of conditions.

RESUME

Grâce à une initiative conjointe des Relevés hydrologiques du Canada et de la Division de l'hydraulique de l'Institut national de recherche sur les eaux, l'étude a pu être menée pour mettre au point un rotor de plastique pour le moulinet hydrométrique Price afin d'en améliorer le plus possible le rendement à basse vitesse. On a fait des ébauches préliminaires à partir d'aspects théoriques et d'essais en bassin de remorquage. On constate que l'on peut atteindre des vitesses limites de moins de 2 cm/s. On prévoit faire d'autres essais exhaustifs pour évaluer la constance du rendement du nouveau rotor dans une plus vaste gamme de conditions.

MANAGEMENT PERSPECTIVE

Improving the Price Current Meter rotor to lower the threshold velocity makes this very useful operational meter more reliable at low water velocities. Repair time and costs of bearing upkeep are also significant results from using a plastic mass-produced rotor. Some investigation of the effect of frazil ice on the plastic rotor, vis a vis the standard metal rotor could be useful.

T. Milne Dick
Chief
Hydraulics Division

PERSPECTIVE-GESTION

L'amélioration du rotor du moulinet hydrométrique Price afin d'abaisser la vitesse limite en fait un courantomètre fonctionnel très utile et plus fiable dans des courants à basse vitesse. Entre autres résultats intéressants, on signale le temps consacré aux réparations et les coûts d'entretien du roulement, lesquels sont réduits à cause de la production massive de rotors de plastique. Il serait cependant utile de mener certaines enquêtres sur l'effet du frasil sur le rotor de plastique par rapport au rotor traditionnel en métal.

Le chef
T. Milne Dick
Division de l'hydraulique

TABLE OF CONTENTS

1.0 INTRODUCTION

The Price Current Meter is the instrument used by the Water Survey of Canada (WSC) to measure stream flow velocities. The rotor of the conventional Price meter consists of an assembly of six conical cups oriented about the vertical axis of rotation and is attached to the frame of the meter as shown schematically in Figure (1). Traditionally, the rotor components have been fabricated out of sheet brass with the whole assembly being protected with chrome or nickel plating, Figure (2a). Recently, because of production costs and quality control of this type of rotor, the United States Geological Survey (USGS) has introduced a plastic rotor which can be mass-produced more cheaply, precisely and quickly using plastic injection moulds, Figure (2b). The WSC wants to adopt a similar strategy and is in the process of developing the necessary mould.

Before designing the mould, the writers attempted to modify the geometry of the conical elements of the USGS rotor in the hope of improving the low speed performance. Such an improvement, if it can be economically incorporated into the mould design, would ensure a better return for the money invested in the mould. Three modifications to the rotor geometry are being considered in this report. The tests were conducted in the towing tank at the National Water Research Institute, Burlington.

2.0 DESIGN CONSIDERATIONS

2.1 Theoretical Analysis

The rotor of the Price meter is an assembly of six conical cups mounted symmetrically about the vertical axis of rotation. The forces which govern the rotation of the rotor are the drag forces on the inside and outside of the cups as well as the resistance due to bearings, gears and contacts in the rotor assembly. These forces create torques about the centre of rotation as shown in Figure 3.

For a given steady flow, the meter rotor turns at a constant rate and therefore the balance of the opposing torques may be written as

$$\frac{1}{2}\rho\, C_{D_1} A(V_1 - \omega r)^2\, r - \frac{1}{2}\rho\, C_{D_2} A(V_2 + \omega r)^2\, r - T = 0 \qquad (1)$$

in which ρ = density of the fluid, A = average "bluff body" area of the cups, V_1 and V_2 are the flow velocity at the open and closed side of the rotor cups respectively, r = effective radius of the rotor as shown in Figure 3, C_{D_1} and C_{D_2} = average drag coefficients for the parts of the rotor exposing the inside and outside of the cups respectively, ω = angular velocity of the rotor and T = the torque due to resistance of bearings, gears and contacts of the rotor assembly. The effect of T is known to be most significant at low velocities and its relative importance decreases as velocity increases (Engel, 1976). For the sake of simplicity, the resisting torque due to the drag on the outside of the cups (designated by subscript 2) and the effect of T may be lumped together to produce a total resisting torque. Equation (1) can therefore be simplified to give

$$C_{D_1}(V_1 - \omega r)^2 - \overline{C_{D_2}}(V_2 + \omega r)^2 = 0 \qquad (2)$$

in which $\overline{C_{D_2}}$ replaces C_{D_2} to reflect the total "lumped" effect of the resisting torque.

When the flow is two-dimensional, the velocity distribution is uniform as shown in Figure 3. This is the case encountered when meters are calibrated in a towing tank. For this type of velocity

distribution $V_1 = V_2 = V$ in which V denotes the velocity at the centre of the rotor. Equation (2) can thus be rearranged to give

$$\omega_0 r = V \left[\frac{\sqrt{C_{D_1}} - \sqrt{C_{D_2}}}{\sqrt{C_{D_1}} + \sqrt{C_{D_2}}} \right] \tag{3}$$

One may also write

$$\omega_0 r = \pi N D \tag{4}$$

in which $\pi = 3.14.....$, N = rate of rotation of the rotor in rev/s when the flow is two-dimensional and D = effective diameter of the rotor (i.e., D = 2r). Substituting equation (4) into equation (3) results in

$$\frac{ND}{V} = \frac{1}{\pi} \left[\frac{\sqrt{C_{D_1}} - \sqrt{C_{D_2}}}{\sqrt{C_{D_1}} + \sqrt{C_{D_2}}} \right] \tag{5}$$

Equation (5) can be further simplified by dividing through by $\sqrt{C_{D_2}}$ to give

$$\frac{ND}{V} = \frac{1}{\pi} \left[\frac{K - 1}{K + 1} \right] \tag{6}$$

in which $K = \sqrt{C_{D_1}} / \sqrt{C_{D_2}}$

It can be seen from Equation (6) that for a given rotor diameter D, the rate of rotation N at a given towing speed V can be changed by changing K.

2.2 Proposed Modifications to Plastic Rotor

An ideal current meter would operate so that the meter rotor would turn through the same number of revolutions per unit length of water, irrespective of the velocity of the meter relative to the water. Such a meter would have a zero threshold velocity and ND/V would be constant at all velocities as shown schematically in Figure 4. In practice, however, current meters experience the effects of fluid frictions on the rotor elements as well as bearing friction, causing considerable slippage at low velocities. As a result ND/V at the lower speeds is not constant but increases as V increases from the threshold value. The amount of slip decreases as the velocity increases and at a certain value of velocity, say V_c, ND/V becomes sensibly constant and independent of velocity (Figure 4). The rate of change in ND/V and the value of V_c are dependent on the magnitude of the threshold velocity. The greater the threshold velocity, the larger the value of V_c at which ND/V becomes constant. This effect is also shown schematically in Figure 4. Obviously, one must strive to obtain a value of V_c for a given meter as low as possible. This can be done by increasing K in Equation (6) and reducing the submerged weight of the rotor to reduce bearing friction (Engel, DeZeeuw, 1984). The effect of this would be to increase the rate of rotation of the rotor for a given velocity, which in turn will reduce the threshold velocity.

The value of K can be increased by increasing C_{D_1} and reducing $\overline{C_{D_2}}$. The parameter $\overline{C_{D_2}}$ represents the combined effect of resistance drag on the rotor elements as well as frictional resistance with the latter largely dependent on the submerged weight of the rotor. For the present investigtion the submerged weight is kept virtually constant and only geometric properties are considered in

order to develop the design dimensions for the plastic injection mold. Therefore, an increase in ND/V for a given V implies an increase in C_{D_1} and/or a decrease in $\overline{C_{D_2}}$ by changing the shape of the conical elements of the U.S.G.S. plastic rotor.

The conical elements of the USGS rotor have flat bases. It has been observed by Engel and DeZeeuw (1981) from tests with conventional metallic rotors having conical cups and rotors in which the cups were sealed with disks providing flat bases to the conical elements, that the rate of rotation for the latter was about 8% slower. Considering that the submerged weight for both cases was virtually the same, the difference in the rate of rotation must be attributed to the difference in C_{D_1}. Data from drag tests given by Hoerner (1965) on hemispherical cups and solids of revolution of identical shape gave values of C_{D_1} = 1.42 and 1.17 respectively. It can be expected that a similar difference exists between conical cups and solid cones. A practical disadvantage of the conical cups is that they tend to accumulate frazil ice during flow measurements under ice covers. Therefore, in order to minimize the collection of frazil ice and at the same time increase C_{D_1} a shallow conical depression in the flat base of the cones having a depth of 6 mm, is proposed.

In reducing the value of $\overline{C_{D_2}}$, emphasis was placed on maintaining the ratio of the height h (base to apex) to base diameter d of the cones. This meant that any change in the shape of the conical elements would be brought about by changing their surface contours. Examination of data by Hoerner (1965) showed that for a cone of a given h/d ratio, the best reduction in the drag coefficient could be obtained by replacing the cone with a parabolic solid of revolution. Such a conversion would give a reduction in the drag coefficient by a factor of 2.4. The cross-section through the base diameter of this parabolic shape is given in Figure 5, together with that of the original conical elements. The data for the parabolic shape given by Hoerner (1965) were obtained for individual isolated bodies in a wind tunnel. One would expect that because of the close proximity of the bluff body elements on the rotor and the rotational motion, the flow

conditions are more complex. Examination of Figure 5 shows that the parabolic cross-secton results in a small increase in volume of each of the bluff bodies. This will reduce the free space between adjacent elements and may thus reduce the potential advantage in drag reduction gained with the parabolic shape. To minimize this problem the parabolic shape was modified and the revised cross-section is also given in Figure 5. It can be seen from Figure 5 that the volume of each parabolic element has thus been reduced by providing a sharper curvature on the nose section.

Given the geometry of the original USGS rotor, the proposed shallow conical depressions in the flat bases of the original conical elements and the new streamlined shape to replace the linear surface of the original cones, there are four possible cases to be examined separately. These are:

*P-1. The original USGS rotor (Figure (6a))
P-2. Shallow depressions only (Figure (6b))
P-3. Flat face and streamlined noses (Figure (6c))
P-4. Shallow depression and streamlined noses (Figure 7a))

The fabricated rotors for case 3 and 4 are shown in Figure 7 and 8. The four cases were tested in the towing tank at the National Water Research Institute in Burlington.

3.0 EXPERIMENTAL EQUIPMENT AND PROCEDURE

3.1 Meter Suspension

The rotors were tested using a Price winter type current meter yoke which was secured to a 20 mm diameter solid steel rod. The assembly was fastened to the rear of the towing carriage.

---

* P denotes plastic rotor.

3.2 Towing Tank

The tank, constructed of reinforced concrete, founded on piles, is 122 metres long and 5 metres wide. The full depth of the tanks is 3 metres, of which 1.5 metres is below ground level. Normally, the water depth is maintained as 2.7 metres. Concrete was chosen for its stability, vibration reduction and to reduce possible convection currents.

At one end of the tank is an overflow weir. Waves arising from towed current meters and their suspensions are washed over the crest, reducing wave reflections. Parallel to the sides of the tank, perforated beaches serve to dampen laterlal surface wave disturbances. The large cross section of the tank also reduces the generation of waves by the towed object.

3.3 Towing Carriage

The carriage is 3 metres long, 5 metres wide, weights 6 tonnes and travels on four precision machined steel wheels.

The carriage is operated in three overlapping speed ranges:

0.5 cm/sec - 6.0 cm/sec
5.0 cm/sec - 60 cm/sec
50 cm/sec - 600 cm/sec

The maximum speed of 600 cm/sec can be maintained for 12 seconds. Tachometer generators conected to the drive shafts emit a voltage signal proportional to the speed of the carriage. A feedback control system uses these signals as input to maintain the constant speed within specified tolerances.

3.4 Data Acquisition

3.4.1 Towing speed

The average speed data for the towing carriage is obtained by recording voltage pulses emitted from a measuring wheel. This wheel is attached to the frame of the towing carriage and travels on one of the towing tank rails, emitting a pulse for each millimeter of travel. The frequency of these pulses is measured using a SBC-100 computer which may in the maximum case store 95000 observations for a given run. The average towing speed computed from this data is accurate to within ±0.1% at the 99% confidence level (Engel, 1985).

3.4.2 Rate of revolution of the rotor

The Price meter is equipped with a contact closure mechanism which gives a voltage pulse for each complete revolution of the rotor. The pulses generated by the rotor are transmitted to a data acquisition module which begins counting the revolutins after the first pulse has been received. This ensures that all the pulses counted represent complete revolutions. In order to obtain the rate of rotation of the rotor in revolutions per second, time is measured simultaneously with the counting of the revolutions using a crystal clock.

3.5 Meter Preparation

Prior to testing, the meter underwent the following inspection:

a) the pentagear was checked to ensure that it was operating freely;
b) the contact wire was cleaned and adjusted for tension to provide good contact;
c) all moving parts were lubricated.

Following the inspection, the meter was hung in a wind tunnel where it was spun for two hours to ensure that all moving parts were "run-in".

3.6 Meter Position

On each test the meter was attached to the rod suspension and lowered into position 30 cm below the water surface. This depth was chosen to avoid surface effects and to create a minimum of drag on the steel suspension rod, thereby reducing undue vibration. In all cases the suspended meter was placed near the centre-line of the towing tank in accordance with test conditions set out by Engel (1977).

3.7 Towing Tests

A tow of the meter with the towing carriage at a pre-set speed was defined as a test. To begin a set of tests, the meter was properly aligned in the specified position. The meter was then towed at different speeds, resulting in a total of about 30 tests up to a maximum of 300 cm/s. Each time the meter was towed, care was taken that steady state conditions prevailed when measurements were recorded. The lengths of the waiting time between successive tests were in accordance with criteria established by Engel and DeZeeuw (1977) or better. For each test, the towing speed, revolutions of the meter rotor, and time were recorded. Water temperatures were not noted since temperature changes during the tests were small and do not affect the meter significantly (Engel, 1976). The data for the tests are given in Tables 1 through 4 inclusive.

3.8 Weight of the Rotors

The weight of each rotor tested was determined in air and in water using standard procedures. The data are given in Table 5.

4.0 DATA ANALYSIS

4.1 Response Curves

Data in Tables 1 to 4 were plotted as N/V (D in ND/V is constant) vs V in Figures 9. In order to facilitate comparisons, average curves were drawn through the plotted points. This effectively reduced the analysis to considerations of the dominant deterministic response of each rotor by removing the small random component. These average curves were then used to compare the effects of the rotor modifications. Superimposed on the plots is the response curve for the conventional metallic Price meter rotor as a reference. This rotor has a constant value of N/V of 1.47 for $V_c \geq 35$ cm/s.

The curve for the original USGS plastic rotor, identified as rotor P-1 in Figure 9(a) shows an increase in N/V with increasing V until at $V = V_c \approx 100$ cm/s $N/V \approx 1.33$. This value of V_c is quite large and considerably larger than the value of $V_c \approx 35$ cm/s observed for the conventional metallic rotor. The shape of the curve in Figure 9(a) is a clear indication of inefficient fluid-rotor coupling and bearing resistance of the rotor.

In Figure 9(b) the curve for rotor P-2 shows the effect that the shallow depression in the flat base of the conical elements has on the rotor response. The variation of N/V with V has now been confined to speeds less than about 40 cm/s. For $V_c \geq 40$ cm/s values of N/V are constant at about 1.37, which is less than the value of 1.47 observed for the conventional metallic rotor. This indicates that the drag force generated by the cones with shallow depressions is smaller than that obtained with the conical cups of the metallic rotor. Nevertheless, relative to the USGS plastic rotor (i.e., rotor P-1), the shallow depressions improve the low speed performance.

In Figure 9(c) the curve for rotor P-3 shows the effect of the streamlined noses, while keeping the flat bases of the conical elements untouched. The curve clearly shows that a further reduction in the value of V_c is achieved with this modification. In this case

N/V becomes constant at about 1.33 when $V_c \approx 17$ cm/s. In comparing the curve with that for rotor P-1 in Figure 9(a), it can be seen that there has been no signiicant increase in N/V. However, the fact that V_c has been reduced from 100 cm/s to about 17 cm/s, gives clear evidence of the low speed improvement as a result of the streamlined noses.

Finally, in Figure 9(d) the curve shows the combined effect of the shallow depression and streamlined noses. The value of V_c has been further reduced to about 10 cm/s above which N/V is constant at a value of 1.38. This value of N/V is still lower than that obtained with the conventional metallic rotor. However, the combined modification have resulted in a response curve which is better than that of the metallic rotor, with the added benefit of providing a lower threshold velocity. The shallow depression provided a slight increase in the constant value of N/V over that obtained with rotor P-3 consisting of flat faces and streamlined noses.

4.2 Threshold Velocities

One of the improvements in the low speed performance sought with the rotor modifications is a significant reduction in the threshold velocity. This velocity, say V_o, is defined as the minimum velocity at which the rotor will revolve at a steady, constant rate. The threshold velocity of the conventional metallic rotor is about 5 cm/s. The rotor performance depends on its geometry and its submerged weight (Engel, DeZeeuw, 1984). However, near the threshold velocity, changes in the submerged weight are probably more significant than changes in geometry. The submerged weight of the USGS plastic rotor is about 2.4 times less than that of the conventional metallic rotor. Therefore, one can expect a lower threshold velocity for the latter. Observations made by Engel and DeZeeuw, 1984, bear this out, giving a value of $V_o = 3.5$ cm/s for the USGS plastic rotor.

The threshold velocities are difficult to determine accurately because of the high degree of uncertainty in the measurement. The values obtained for the modified plastic rotors are single values and need to be confirmed by additional testing. The threshold values obtained are given in Table 6. The data show that there is a tendency toward significant reduction in the threshold velocity with the P-4 rotor. A value of less than 2.0 cm/s for a mechanical meter must be considered to be very good. In comparison, magnetic flow meters such as the Marsh McBirney have a threshold at about 1 cm/s (Engel and DeZeeuw, 1981). However, before final conclusions can be made, more tests using several rotors should be used.

4.3 Linear Regression Equations

It is the present practice to perform linear regressions on the calibration data to obtain calibration equations of the form

$$V = a + bN \quad \ldots\ldots\ldots \quad (7)$$

where "a" is an intercept and "b" is the slope of the equation. Theoretically, if the meter behaves like an ideal meter for which $V_o = 0$, then $a = 0$. However, because of friction in the bearings and contacts, $V_o > 0$ and thus the value of "a" depends largely on the magnitude of V_o. However, "a" is always less than V_o so that $a/V_o < 1$. As V_o becomes smaller one expects "a" to become smaller but this also depends on the slope "b" of the equation. The relative relationship between "a", "b" and V_o is shown schematically in Figure 10. Regression equations for each of the four rotor cases were obtained together with their coefficient of correlation "r", standard errors of estimates, "S_E", and these are given in Table 7.

Examination of Table 7 shows that for rotors P-1 and P-2 the data could be fitted by a single equation. In contrast to this for rotors P-3 and P-4 two equations were required. Over the same speed

range or $10 \leq V \leq 300$ cm/s. In each of the latter two cases, the two equations intersect at virtually the same velocity of 215 cm/s. It is most probable that the change in slope in the calibration is due to the presence of the streamlined noses on the conical elements. The exact reason for this is not clear, but is is possible that the flow regime around the rotor elements has been effected sufficiently by the reduction in the spaces between successive streamlined elements. This resulted in slightly smaller slopes for the equation in the upper speed range (i.e., $V > 215$ cm/s).

Examination of the standard errors of estimate S_E shows that the largest value occurs for the original USGS rotor. Values of S_E for rotor P-2 and those for the second equations of rotors P-3 and P-4 are approximately the same with the lowest value occurring for P-3. For the first equations of rotors P-3 and P-4 the standard errors of estimates are virtually the same. Examinations of the intercepts of the equations for rotors P-1 and P-2 and those for the equations of the lower speed range for rotors P-3 and P-4 show that in the latter two cases, "a" is much lower. This reflects the low threshold velocities obtained with the P-3 and P-4 rotors.

Considering the low speed and high speed performance, both the P-3 and P-4 rotor give a significant improvement over the original USGS rotor. In order to decide which one of these two rotors should be developed, additional tests need to be conducted. Such tests should be made with several rotors over a wide range of conditions including the effects of horizontal and vertical deviation from true alignment.

5.0 CONCLUSIONS AND RECOMMENDATION

1. The performance of the USGS plasic rotor can be significantly improved by making prudent changes in the rotor geometry.

2. Streamlined noses on the rotor elements tend to increase the linearity in the rotor's low speed response. With this type of modification two separate calibration equations for low and upper speed range are required. Preliminary results indicate that the point of intersection of these equations is near a velocity of 215 cm/s.
3. Depressions in the bases of the conical rotor elements increases the rate of rotation of the rotor by about 4%.
4. Rotors P-3 and P-4 provide significant improvement over the original USGS rotor. Preliminary results show that threshold velocities of less than 2 cm/s can be obtained. Further tests are required to determine which of the two rotors will be adopted as the prototype to develop an injection mould. Such tests should be conducted using several rotors over a wide range of speeds including horizontal and vertical deviations from true alignment.
5. Care should be taken in measuring the threshold velocity since this parameter may be the deciding factor in choosing the final design.

ACKNOWLEDGEMENTS

The writers are particularly indebted to G. Voros who was responsible for the fabrication of the test rotors. The care and dedication of C. Bil and B. Near who conducted the towing tests is also much appreciated.

REFERENCES

Engel, P. 1976. A Universal Calibration Equation for Price Meters and Similar Instruments. Scientific Series No. 65, Inland Waters Directorate, CCIW, Burlington, Ontario.

Engel P. and C. DeZeeuw. 1977. Determination of Waiting Times Between Successive Runs When Calibrating Price 622AA Type Current Meters in a Towing Tank. Technical Note, Hydraulics Research Division, Canada Centre for Inland Waters, Burlington Ontario.

Engel, P. 1977. An Experimental Outline to Study the Performance of the Price Current Meter. Unpublished Manuscript, Hydraulics Research Division, CCIW, Burlington, Ontario.

Engel P., C.N. DeZeeuw. 1980. Performance of the Price 622AA, OTTC-1 and Marsh-McBirney 201 Current Meters at Low Speeds. Technical Note No. 80-14, Hydraulics Divison, NWRI, Burlington.

Engel, P. and C. DeZeeuw. 1981. Sensitivity of the Price Current Meter to the Effects of Frazil Ice. Technical Note No. 81-25, Hydraulics Divison, National Water Research Institute, Burlington, Ontario.

Engel, P. and C. DeZeeuw. 1984. On the Effect of Changes in Geometry and Submerged Weight of the Price Meter Rotor. Unpublished Manuscript, Hydraulics Division, NWRI, Burlington, Ontario.

Engel, P. 1985 Calibration of Current Meters for Turbine Efficiency Tests. Unpublished Manuscript, Hydraulics Division, National Water Research Institute, Burlington, Ontario.

Hoerner, S.F. 1965. Fluid-Dynamic Drag. Published by the Author, Library of Congress Catalogue Card Number 64-19666, U.S.A.

TABLE 1

Data for USGS Plastic Rotor P-1

Test	V cm/s	N rev/s	N/V rev/m
1	5.01	0.0595	1.187
2	10.06	0.1290	1.282
3	20.06	0.2625	1.303
4	29.99	0.3738	1.247
5	40.31	0.5260	1.305
6	50.17	0.6610	1.318
7	60.28	0.7913	1.313
8	70.50	0.9350	1.326
9	79.74	1.0560	1.324
10	90.22	1.2022	1.333
11	100.32	1.3444	1.340
12	110.64	1.4810	1.339
13	119.74	1.6000	1.336
14	129.94	1.7361	1.336
15	140.20	1.8702	1.334
16	150.26	2.0028	1.333
17	160.81	2.1450	1.334
18	170.69	2.2779	1.335
19	180.49	2.4062	1.333
20	190.46	2.5336	1.330
21	200.45	2.6738	1.334
22	209.98	2.7925	1.330
23	220.61	2.9386	1.332
24	230.22	3.0779	1.337
25	240.69	3.2216	1.339
26	250.66	3.3580	1.340
27	260.81	3.4868	1.337
28	271.13	3.6101	1.332
29	280.80	3.7425	1.333
30	289.53	3.8491	1.329
31	300.78	4.0032	1.331

TABLE 2

Data for Modified Rotor P-2

Test	V cm/s	N rev/s	N/V rev/m
1	2.02*	0.232	1.147
2	3.01	0.358	1.191
3	4.01	0.0496	1.237
4	5.03	0.0625	1.243
5	6.01	0.0745	1.240
6	7.14	0.0935	1.309
7	8.13	0.1030	1.267
8	9.14	0.1167	1.277
9	10.16	0.1319	1.249
10	15.09	0.2032	1.347
11	20.18	0.2715	1.345
12	25.12	0.3404	1.355
13	30.12	0.4047	1.344
14	35.16	0.4730	1.345
15	40.14	0.5522	1.376
16	45.06	0.6125	1.359
17	50.15	0.6848	1.366
18	60.08	0.8208	1.366
19	70.61	0.9597	1.359
20	80.27	1.0969	1.367
21	90.44	1.2361	1.367
22	100.52	1.3689	1/362
23	110.08	1.4979	1.361
24	120.49	1.6420	1.363
25	140.56	1.9102	1.359
26	160.32	2.1782	1.359
27	180.72	2.4588	1.361
28	200.25	2.7315	1.364
29	221.51	3.0157	1.361
30	240.53	3.283	1.365
31	260.72	3.5562	1.364
32	280.27	3.8241	1.364
33	300.44	4.0933	1.362

* Threshold

TABLE 3

Data for Modified Rotor P-3

Test	V cm/s	N rev/s	N/V rev/m
1	2.02*	0.180	0.892
2	3.01	0.0343	1.139
3	4.05	0.0472	1.166
4	5.03	0.0630	1.252
5	6.06	0.0773	1.276
6	7.09	0.0926	1.306
7	8.17	0.1046	1.280
8	9.18	0.1184	1.290
9	10.13	0.1295	1.279
10	15.06	0.2004	1.331
11	20.05	0.2668	1.331
12	25.07	0.3322	1.325
13	30.09	0.3954	1.314
14	35.05	0.4664	1.331
15	40.08	0.5313	1.326
16	45.17	0.6026	1.334
17	50.16	0.6641	1.324
18	60.17	0.8016	1.332
19	70.82	0.9368	1.323
20	80.52	1.0633	1.324
21	90.25	1.1900	1.319
22	100.39	1.3228	1.318
23	110.24	1.4562	1.321
24	120.57	1.5924	1.321
25	140.71	1.8594	1.322
26	161.02	2.1281	1.322
27	180.40	2.3827	1.321
28	200.49	2.6497	1.322
29	220.74	2.4206	1.323
30	240.27	3.1857	1.326
31	260.32	3.4542	1.327
32	280.56	3.7383	1.332
33	300.64	4.0016	1.331

* Threshold

TABLE 4

Data for Modified Rotor P-4

Test	V cm/s	N rev/s	N/V rev/m
1	1.53*	0.0110	0.717
2	2.02	0.0197	0.974
3	3.01	0.0351	1.166
4	4.05	0.0503	1.243
5	5.03	0.0655	1.303
6	6.06	0.0818	1.349
7	7.09	0.0972	1.370
8	8.17	0.1103	1.350
9	9.18	0.1245	1.356
10	10.13	0.1365	1.347
11	15.06	0.2090	1.388
12	20.05	0.2784	1.388
13	25.07	0.3471	1.385
14	30.09	0.4133	1.374
15	35.05	0.4880	1.392
16	40.08	0.5520	1.377
17	45.17	0.6271	1.388
18	50.16	0.6920	1.380
19	60.17	0.8335	1.385
20	70.82	0.9766	1.379
21	80.52	1.1093	1.378
22	90.25	1.2358	1.369
23	100.39	1.3819	1.377
24	110.24	1.5135	1.373
25	120.57	1.6537	1.372
26	140.71	1.9286	1.371
27	161.02	2.2099	1.373
28	180.40	2.4759	1.372
29	200.49	2.7556	1.374
30	220.74	3.0386	1.377
31	240.27	3.3003	1.374
32	260.32	3.5842	1.377
33	280.56	3.8775	1.382
34	300.64	4.1684	1.387

* Threshold

TABLE 5

Weight in Air and Water for Tested Rotors

Rotor	Weight in Air (Newtons)	Weight in Water (Newtons)
1. U.S.G.S	1.98	0.52
2. Conical Depression in Flat Cone Base	1.73	0.46
3. Curvilinear Nose and Flat Face	2.40	0.57
4. Curvilinear Nose and Conical Depression	2.16	0.57

TABLE 6

Threshold Velocities

Rotor Type	V_o cm/s
Conventional Metallic	5.0
U.S.G.S. Plastic (P-1)	3.5
P-2	2.0
P-3	2.0
P-4	1.5

TABLE 7

Regression Equations

Rotor Type	Slope, "b" cm/rev	Intercept, "a" cm/s	SE cm/s	r	Speed Range cm/s
P-1	74.80	0.57	0.58	0.999	$10 \leq V \leq 300$
P-2	73.17	0.37	0.34	0.999	$10 \leq V \leq 300$
P-3	75.69	-0.01	0.18	0.999	$10 \leq V \leq 215.3$
	73.48	6.28	0.29	0.999	$215.3 \leq V \leq 300.0$
P-4	72.91	-0.17	0.21	0.999	$10 \leq V \leq 215.7$
	70.68	6.41	0.40	0.999	$215.7 \leq V \leq 300.0$

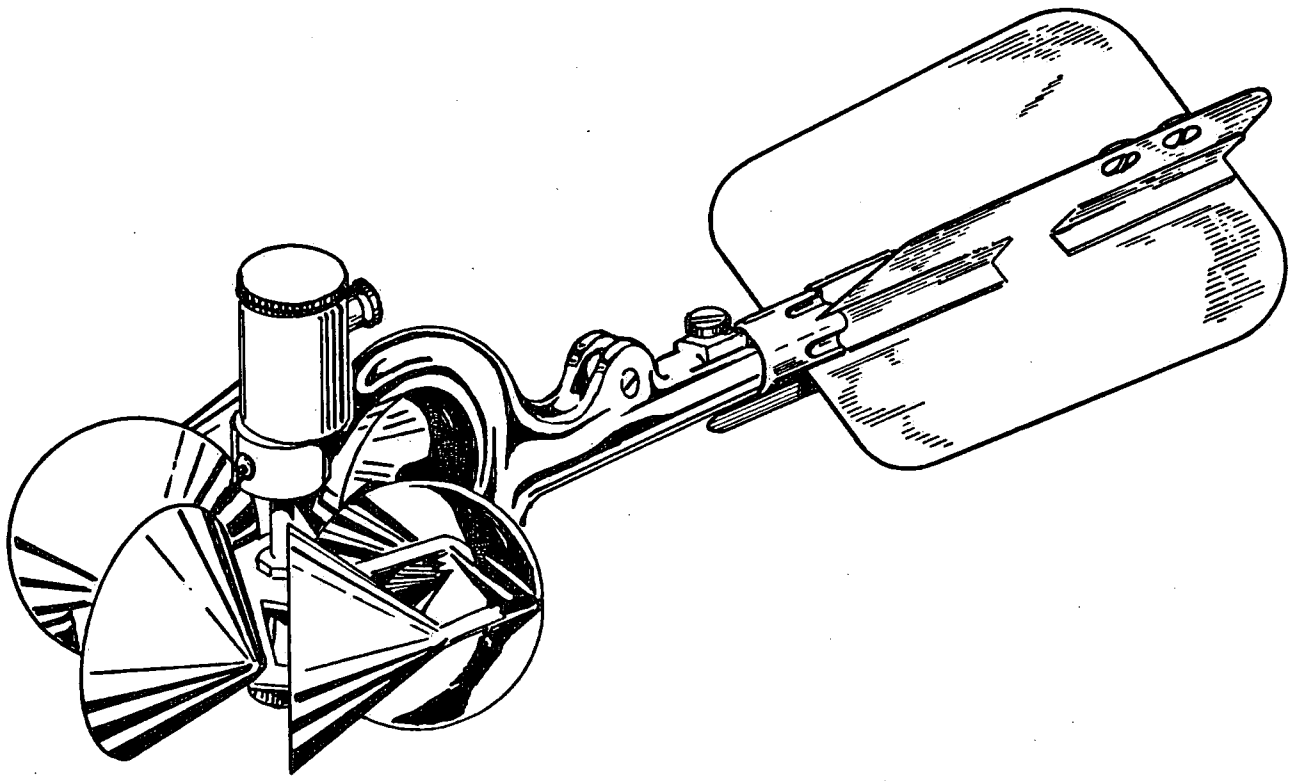

FIGURE 1. PRICE METER WITH CONVENTIONAL ROTOR

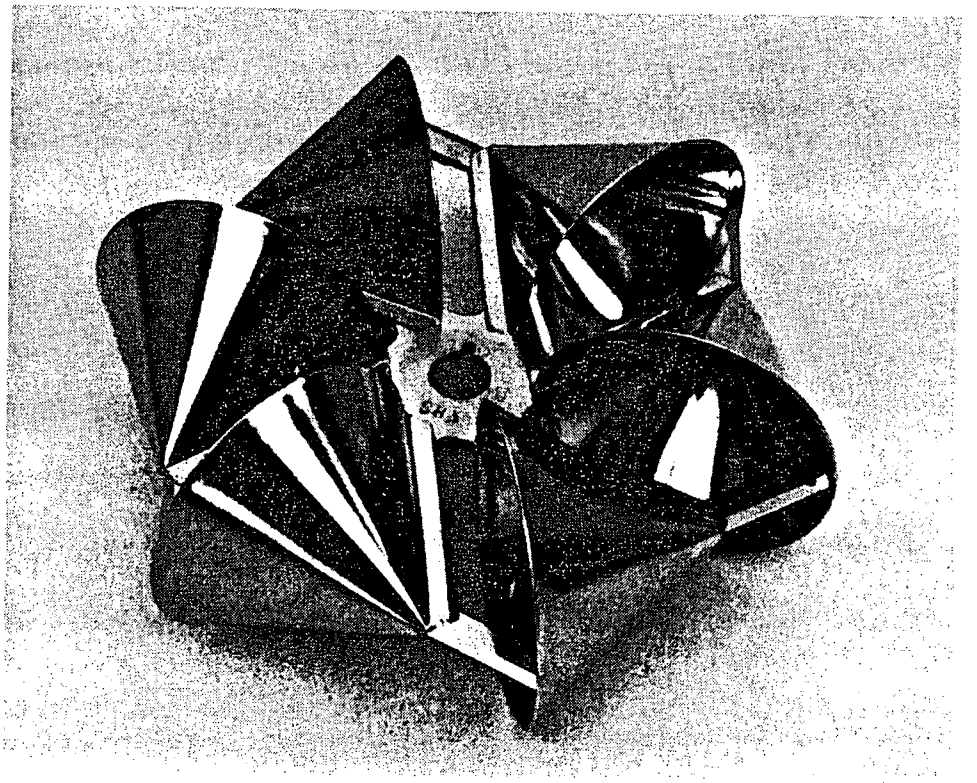

FIGURE 2a. CONVENTIONAL ROTOR

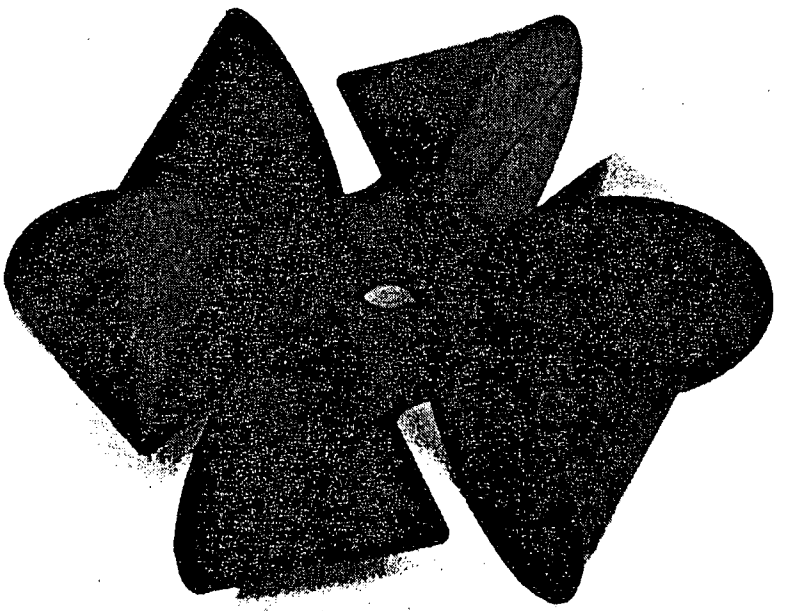

FIGURE 2b. PLASTIC ROTOR

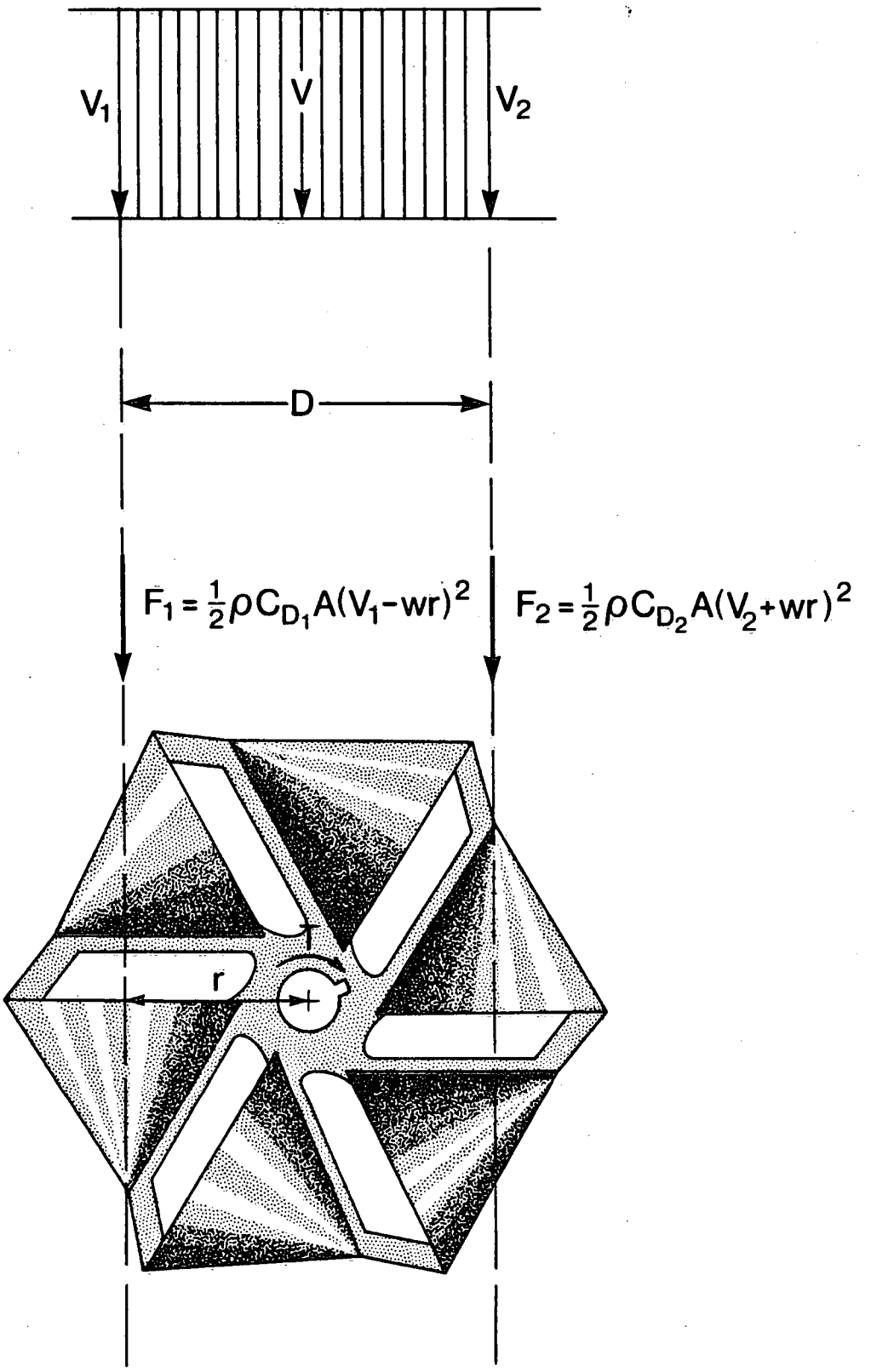

FIGURE 3. VELOCITY DISTRIBUTION FOR TWO DIMENSIONAL FLOW RELATIVE TO METER ROTOR

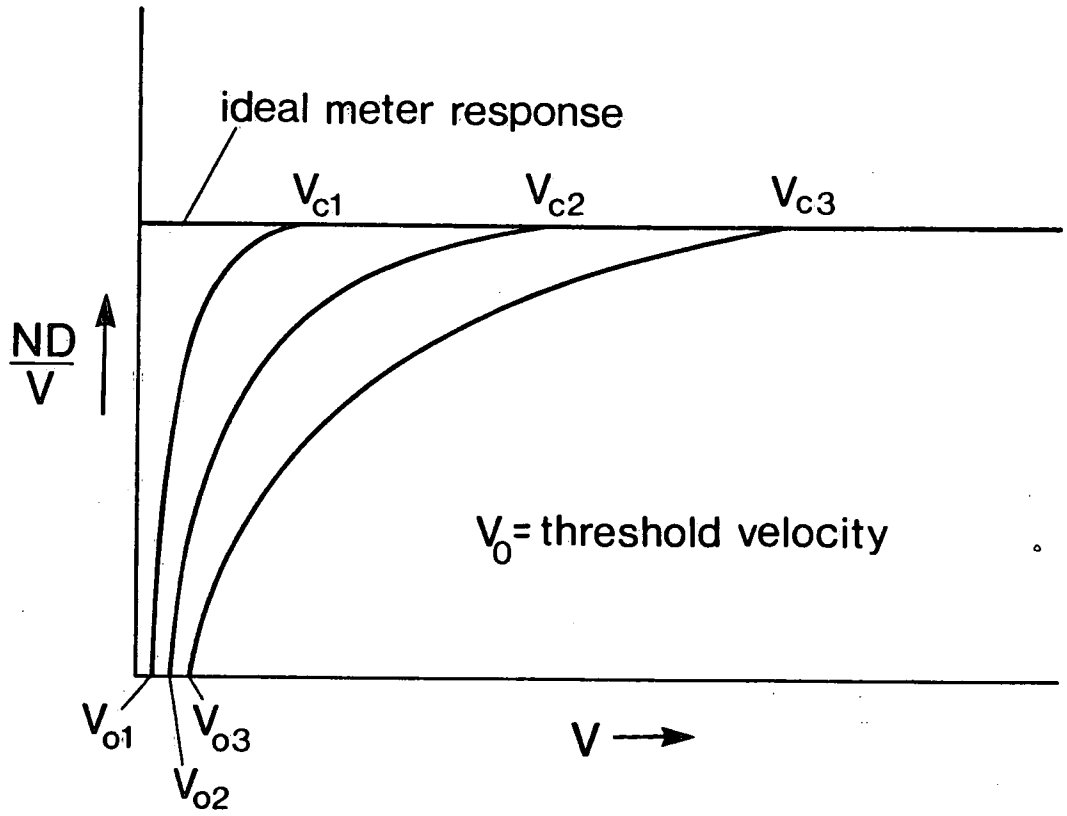

Figure 4 Rotor Response Curves for Different Threshold Velocities

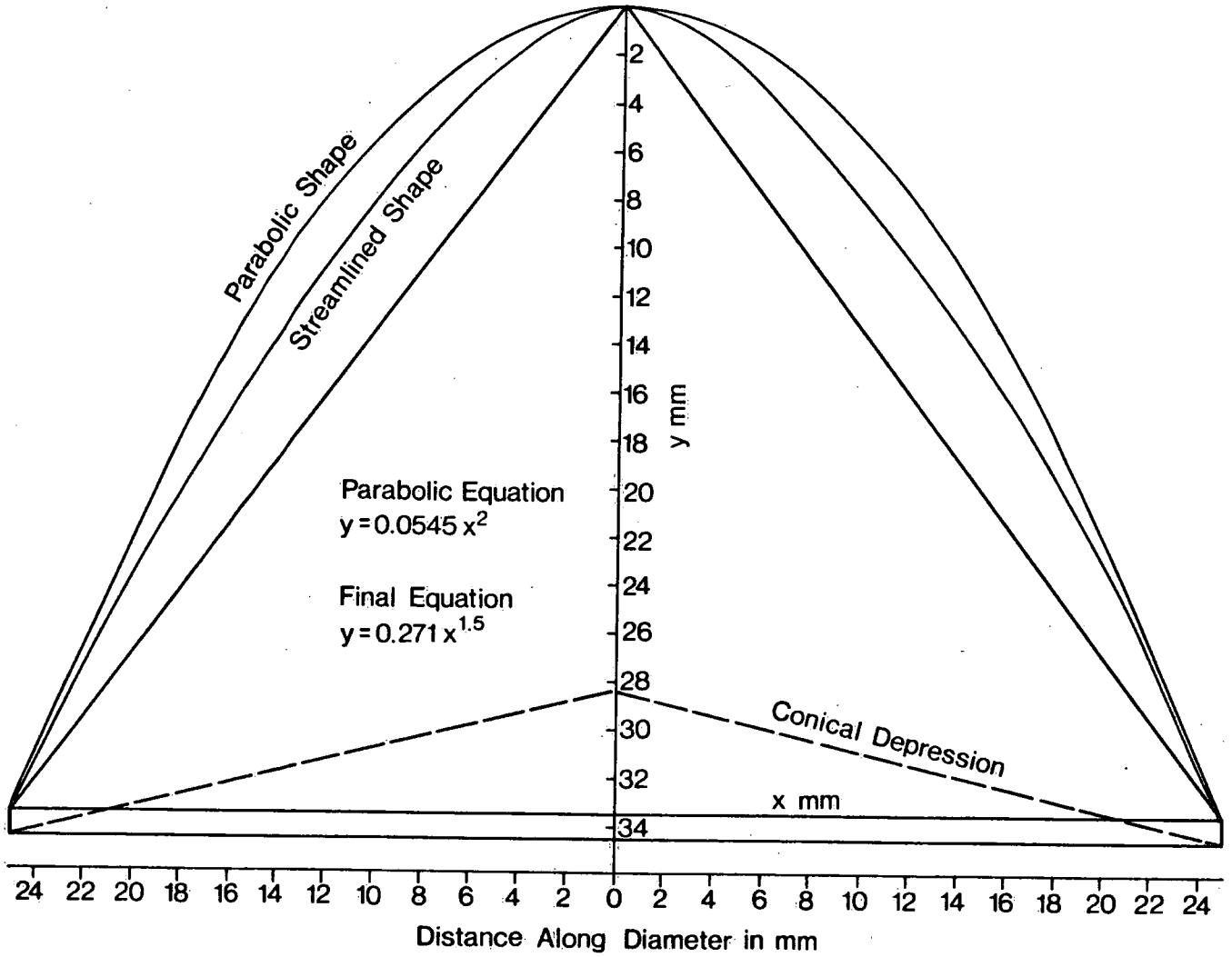

Figure 5 Crossections of Rotor Elements

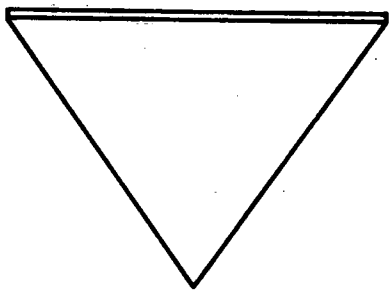

a) ROTOR P-1

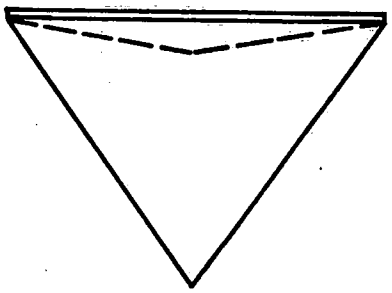

b) ROTOR P-2

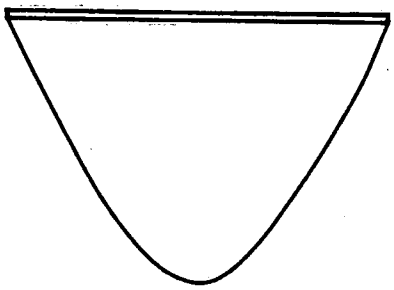

c) ROTOR P-3

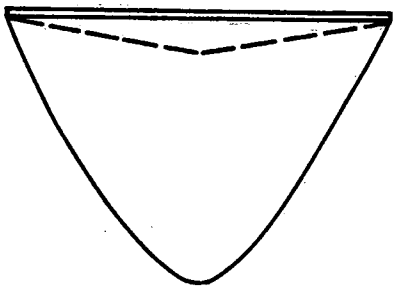

d) ROTOR P-4

Figure 6 Shapes of Rotor Elements Tested

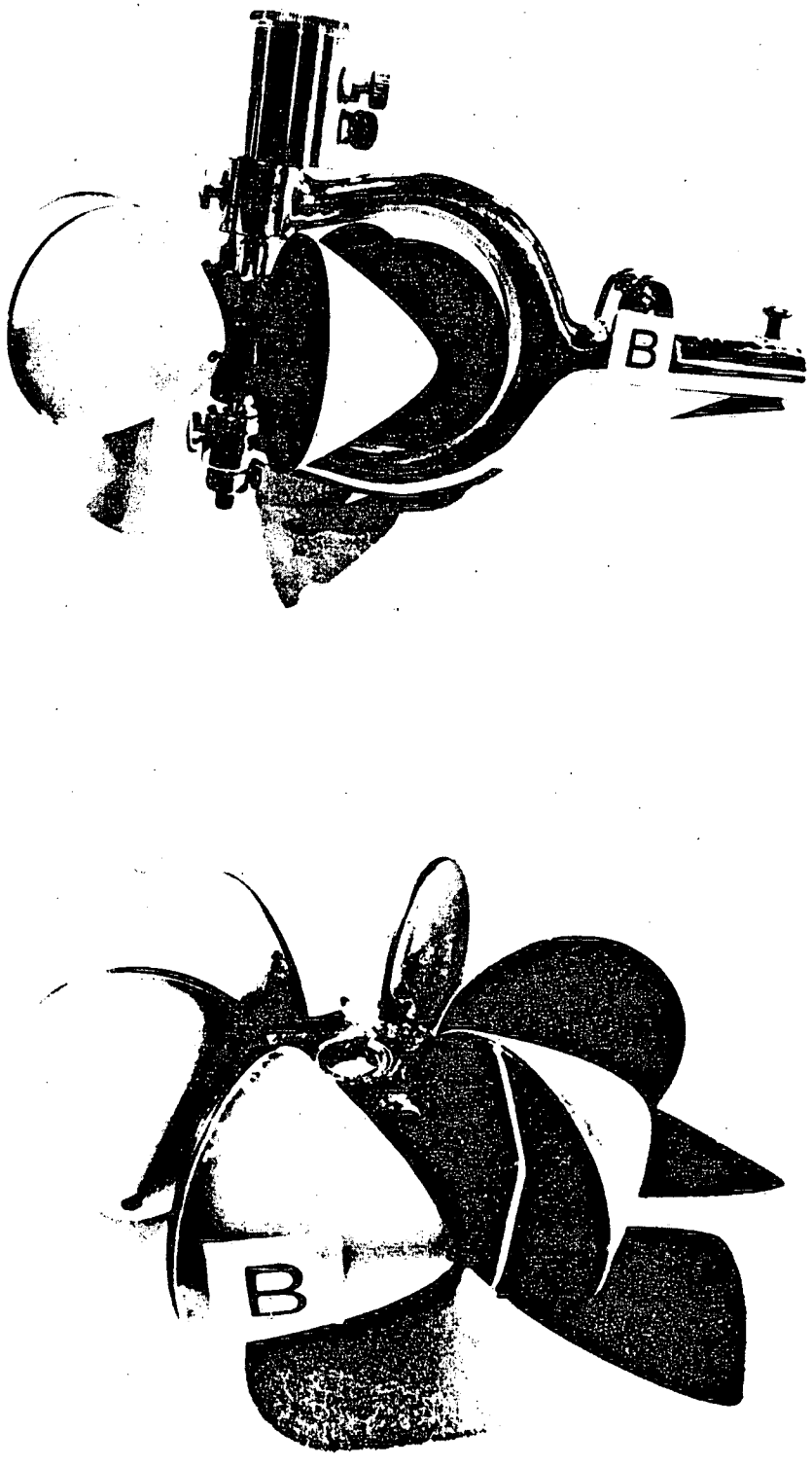

Figure 7 Rotor with elements having depressed face and streamlined nose.

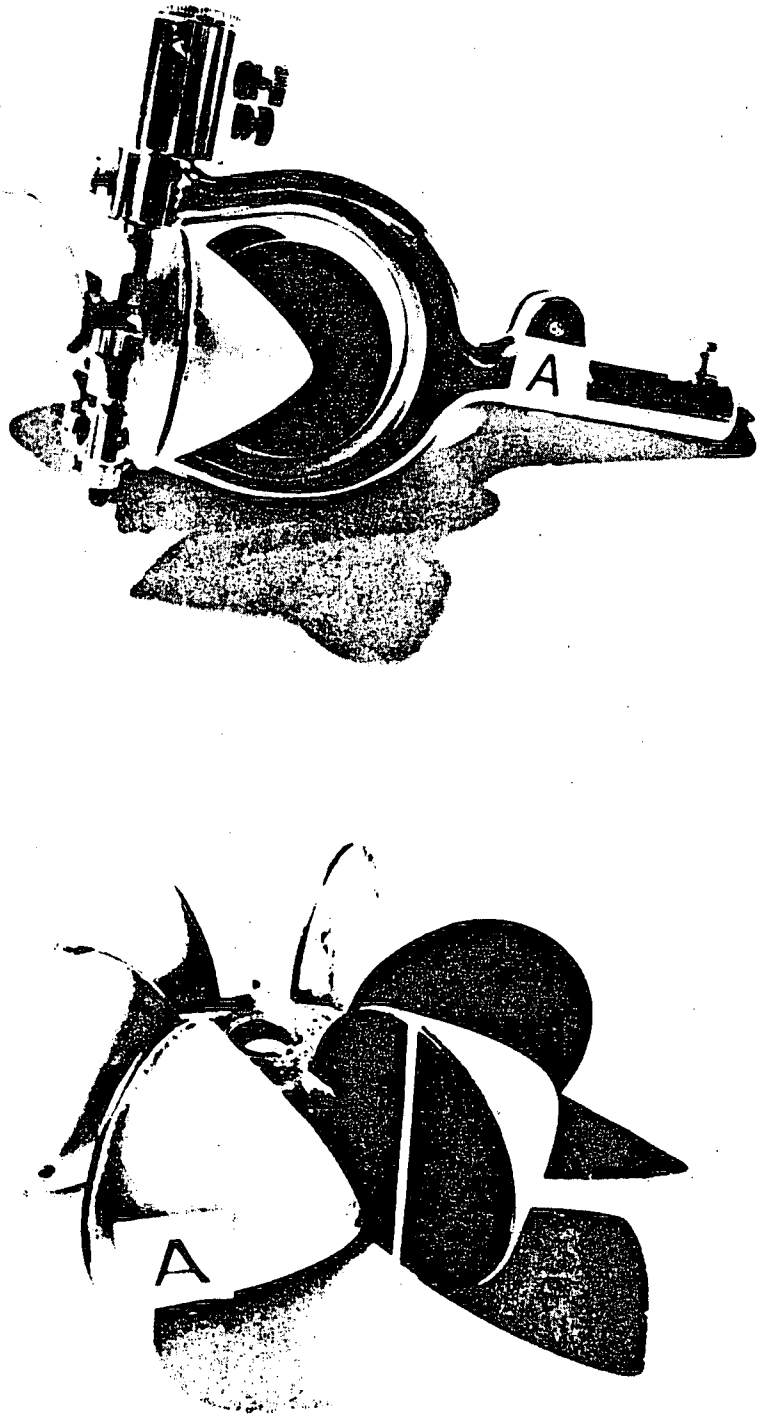

Figure 8 Rotor with elements having flat face and streamlined nose.

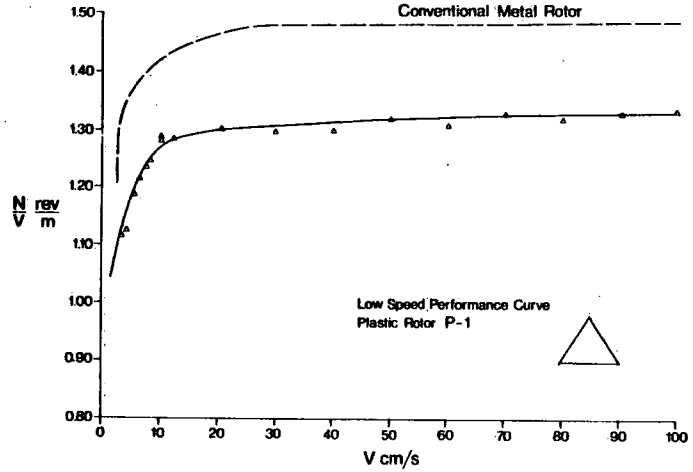

a) U.S.G.S. Rotor (P-1)

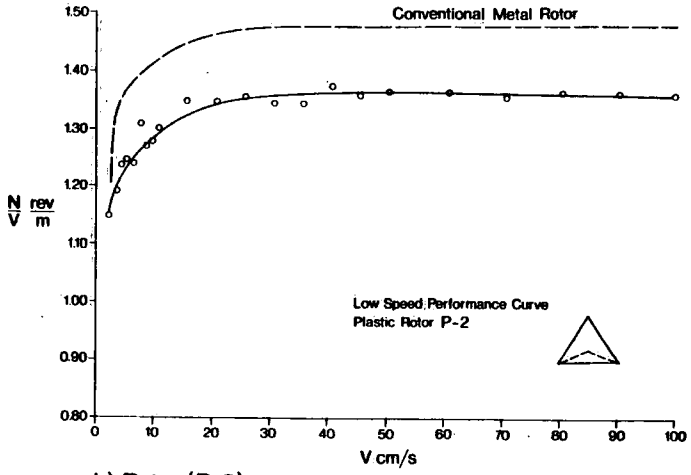

b) Rotor (P-2)

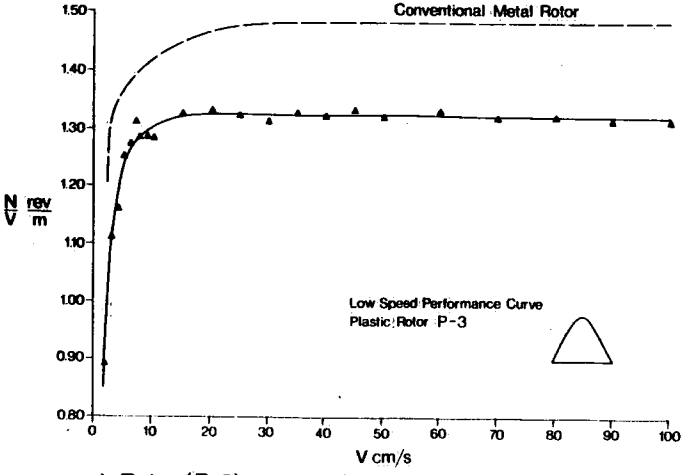

c) Rotor (P-3)

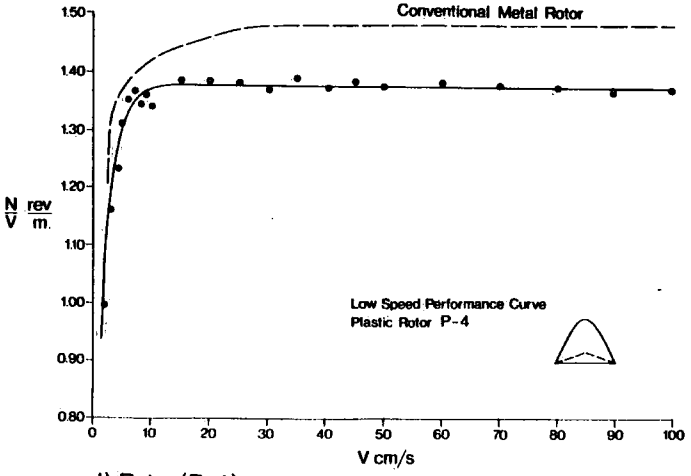

d) Rotor (P-4)

Figure 9 Response Curves for U.S.G.S. Rotor and Tested Modifications

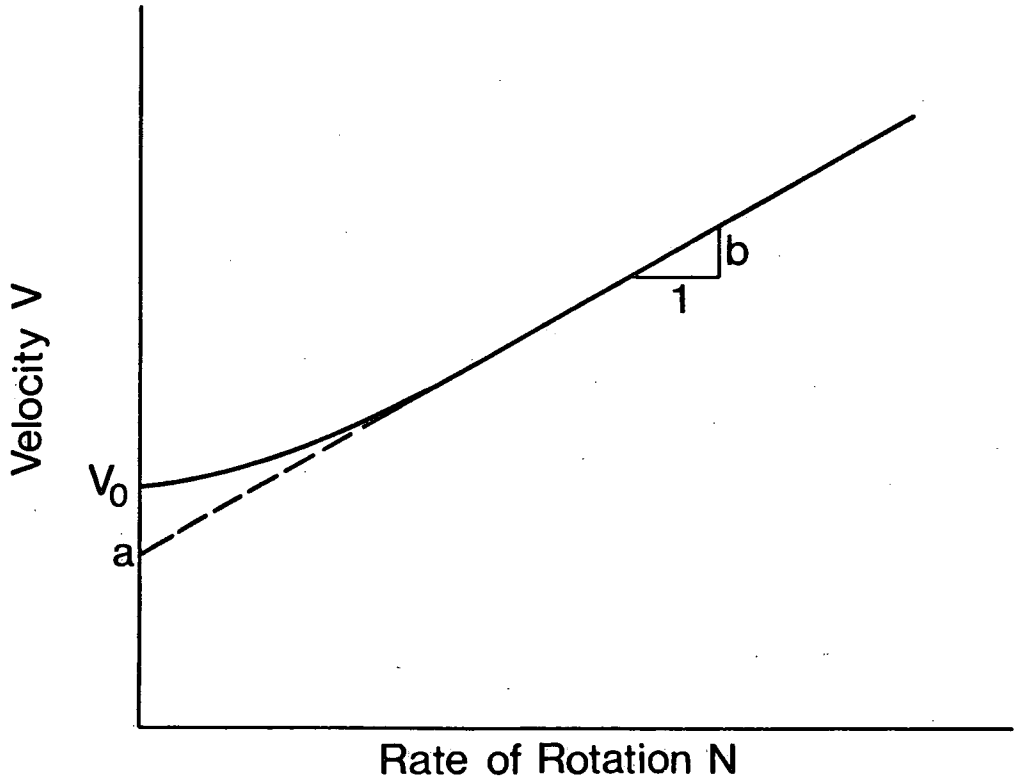

Figure 10 Definition of V_0, a and b